Coordinated Demand Response of Rail Transit Load and Energy Storage System Considering Driving Comfort

Hongming Yang, *Member, IEEE*, Wangda Shen, Qian Yu, Junpeng Liu, Yizhe Jiang, Emmanuel Ackom, and Zhao Yang Dong, *Fellow, IEEE*

***Abstract*—Electric trains typically travel across the railway networks in an inter-provincial, inter-city and intra-city manner. The electric train generally serves as a load/source in tractive/brake mode, through which power networks and railway networks are closely coupled and mutually influenced. Based on the operational mode of rail trains and the characteristics of their load power, this paper proposes a coordinated optimal decision-making method of demand response for controllable load of rail trains and energy storage systems. First, a coordinated approach of dynamically adjusting the load of the controllable rail train in considering the driving comfort and energy storage battery is designed. Secondly, under the time conditions that satisfy the train's operational diagram, the functional relationship between the train speed and the load power is presented. Based on this, in considering the constraints of the train's arrival time, driving speed, motor power, and driving comfort, the capacity of energy storage batteries and other constraints, an optimization model for demand response in managing the traction power supply system under a two-part price and time-of-use (TOU) price is proposed. The objective is to minimize the energy consumption costs of rail transit trains, and optimize the speed trajectory of rail trains, the load power of traction system, and the output of energy storage batteries.**

***Index Terms*—Controllable traction load, demand response, driving comfort, energy storage battery, rail train, speed trajectory.**

NOMENCLATURE

Abbreviations

TOU	Time-of-use.
SOC	State of charge.

Indices and Set

i	Train.
t	Time instant.
n	Bus.
m	Section in the rail transit network.
l	Transmission line in the power grid.
M	The total number of sections.
V	The set of all sections in the rail transit network.
Γ_{D}	The set of sections belonging to stations.
Ω_n	The train set in power supply interval.
Γ_n	The set of all sections within the jurisdiction of the power supply interval n.

Parameters

η	The energy conversion efficiency.
$P_{i,\mathrm{aux}}$	The loading power of auxiliary facilities for train i.
u_{f}	The tractive effort coefficient of the train.
E_i	The voltage of traction network on which train $i$is located.
u_{b}	The braking force coefficient of the train.
$a^{\mathrm{r}}, b^{\mathrm{r}}, c^{\mathrm{r}}$	The coefficient set by the train types and marshaling method.
q	The thousand fraction of the ramp, i.e. the ratio of elevation difference and horizontal distance between the two ends of the ramp.
E	The voltage of the low voltage side of the traction substation.
V_i	The voltage of train i.
$I_{i,t}$	The electric current of train i.
R	The radius of the curve.
$P_{\mathrm{R},n,\max}$	The maximum loading power limit of the traction substation on node.
$v_{\max}$	The maximum speed limit of the train.
$a_{\min}, a_{\max}$	The minimum and maximum acceleration rates of the train, respectively.
g	The acceleration of gravity.
D	The distance between two rails on a railway.
H	The superelevation of the plane curve.
$R_{\mathrm{H}}, R_{\mathrm{s}}$	The radius of the plane curve and the vertical curve.
L_{H}, L	The length of plane curve and track line, respectively.

Manuscript received June 9, 2020; revised July 9, 2020; accepted July 28, 2020. Date of online publication August 19, 2020; date of current version August 25, 2020. This work was supported in part by the National Natural Science Foundation of China (71931003), the Science and Technology Projects of Hunan Province and Changsha City (2018GK4002, 2019CT5001, 2019WK2011, 2019GK5015 and kq1907086).

H. M. Yang (corresponding author, e-mail: yhm5218@163.com), W. D. Shen, J. P. Liu and Y. Z. Jiang are with Hunan Provincial Engineering Research Center for Electric Transportation and Smart Distribution Network, International Joint Laboratory of Ministry of Education for Operation and Planning of Energy Internet based on Distributed Photovoltaic-Storage Energy, School of Electrical and Information Engineering, Changsha University of Science & Technology, Changsha 410114, China.

Q. Yu is with the School of Economics and Management, Changsha University of Science & Technology, Changsha 410114, China.

E. Ackom is with UNEP DTU Partnership, Technical University of Denmark, 2100 Copenhagen, Denmark.

Z. Y. Dong is with the School of Electrical and Engineering and Telecommunications, University of New South Wales, Sydney, NSW, 2052, Australia.

DOI: 10.17775/CSEEJPES.2020.02590

L_{s} The length of vertical curve.
T The operating period of the rail transit system, generally 24 hours a day.
k The operation and maintenance cost of the energy storage battery to charge and discharge the unit power.
e_{t} The TOU power price at time instant t.
e_{s} The capacity price.
e_{z} The penalty price for the excess when the load of the rail transit exceeds the maximum demand reported by the power grid.
S The maximum demand reported by the power grid.
$P_{\mathrm{E},n}^{\max}, P_{\mathrm{E},n}^{\min}$ The maximum and minimum output power of the energy storage battery on node n, respectively.
$S_{n,\min}^{\mathrm{SOC}}$ The minimum SOC of the energy storage battery on node n.
$S_{n,\max}^{\mathrm{SOC}}$ The maximum SOC of the energy storage battery on node n.
$P_{\mathrm{l}}^{\max}$ The maximum transmitted power of line l.

Variables

$P_{\mathrm{R},i,t}$ The loading power of train i at time instant t.
$F_{\mathrm{q},i,t}, F_{\mathrm{b},i,t}$ The tractive effort and braking force of train i at time instant t, respectively.
$f_{i,t}, w_{i,t}$ The basic resistance and additional resistance of train i at time instant t, respectively.
$v_{i,t}$ The traveling speed of train i at time instant t.
$w_{i,\mathrm{q}}$ The ramp resistance of train i.
$w_{i,\mathrm{r}}$ The curve resistance of train i.
$w_{i,t}$ The additional resistance of train i at time instant t.
$P_{\mathrm{R},n,t}$ The loading power of traction substation at time instant t on node n.
$v_{i,m}, v_{i,m'}$ The driving speed of train i to sections m and m', respectively.
$L_{m,m'}$ The distance between sections m and m'.
$a_{i,m,m'}$ The uniform acceleration of train i between sections m and m'.
$a_{i,m}$ The uniform acceleration of train i to section m.
$t_{i,\mathrm{start}}$ The starting time of train i.
s_i The section number when train i departs.
$\Delta T_{i,m}$ The dwell time on station m.
$\bar{v}_{i,m,m'}$ The average driving speed between station sections m and m'.
$T_{i,m}$ The arrival time of train i planned by timetable at station section m.
$a_{\mathrm{LX1},i,m}$ The centrifugal acceleration suffered by train i when passing through the plane curve of section m.
$a_{\mathrm{LX2},i,m}$ The vertical centrifugal acceleration suffered by train i when passing through the vertical curve of section m.
$\beta_{\mathrm{HX},i,m}$ The lateral comfort of train i.
$\beta_{\mathrm{CX1},i,m}$ The vertical comfort caused by centrifugal acceleration.
$\beta_{\mathrm{CX2},i,m}$ The vertical comfort caused by centrifugal acceleration.
$P_{\mathrm{E},n,t}$ The charging or discharging power of the energy storage battery at time instant t on node n.
$P_{\mathrm{G},n,t}$ The power from the grid at time instant t on node n.
$S_{n,t}^{\mathrm{SOC}}$ The SOC of the energy storage battery at time instant t.
$S_{n,t-1}^{\mathrm{SOC}}$ The SOC of the energy storage battery at time instant $t-1$.
Δt The time interval of the charging/discharging of the energy storage battery.
$B_{n,\mathrm{E}}^{\mathrm{Cap}}$ The capacity of the energy storage battery on node n.
P_{l} The transmitted power of the line l.

I. Introduction

With the ever-increasing urban population, the scale continues to expand, traffic congestion is further highlighted, and electrified rail traffic has become an important development direction of modern public transportation networks [1]. At the end of 2018, China had 185 track operation lines in 35 cities, with an operating mileage of 5,761.4 km; intercity and interprovincial high-speed railways operated 29,000 km [2]. The development of rail transportation allows for the needs of people to travel quickly, and the huge energy consumption problem caused by the use of electricity cannot be ignored. In 2016, the nation's electrified railways consumed 60 billion kW·h of electricity, and Beijing, Shanghai, and Guangzhou subway loads accounted for 1.5% to 2.5% of the city's total load, becoming the largest single load in the city [3]. In order to cope with the overload of the urban rail transit power supply system during peak commuting hours, a large number of energy storage devices are installed in the rail traction power supply system as an effective means to suppress load fluctuations [4]–[6].

Rail transit, as the first-level load of the power system, primarily comprises the energy consumption of the traction system required by the train during the driving process, and the energy consumption of auxiliary systems required to ensure the normal operation of the train, such as ventilation, air conditioning, lighting, etc. These two types of electricity consumption account for 80% and 20% [7]. Traction power supply is generally composed of a three-phase AC system and a DC power supply system, and the two are electrically connected through a traction substation. When the train is in the traction mode, the traction motor will be switched to electric mode, in which the train absorbs electrical energy from the traction network and converts it into kinetic energy. When the train is under regenerative braking conditions, the electric mode of the traction motor will be changed to the power generation mode, where the kinetic energy generated by the deceleration of the train is converted into electrical energy and fed back to the DC traction network [8], [9].

Rail trains travel between the adjacent stations according to the planned operational diagram. When a given train arrives

at each station at the departure time and arrival time, by optimizing the combined operating conditions of accelerating, cruising and braking, the driving speed trajectory of the train is adjusted in time, thereby changing the traction power required by the train [10], [11]. In [12], by controlling the train's operating conditions and optimizing its driving schedule, a dynamic energy-saving train optimization method, with the goal of minimum traction energy consumption and minimum running time, based on dynamic programming is proposed. In [13], with the objective of minimizing the traction energy consumption and travel time, a multi-objective optimization model of speed trajectory is established subject to the operating safety requirements, passenger comfort and dynamic performance of the trains.

In the process of rail train operations, the traveling comfort of the customer has become an essential point in improving the rail transit services and expanding the market [14]. In [15], the reported method is to improve the comfort level of the train by controlling the driving speed under different operating conditions, whereas the quantitative calculation method of the driving speed and comfort level of train is not given. In [16], a comfort evaluation model is constructed by considering the influence of the track line parameters, in which only the train driving speed and line parameters are considered. The effects of load power of multiple trains on driving speed are neglected. The above-mentioned research primarily focuses on the optimization of mechanical energy consumption, operating speed, and comfort level for single train driving needs. Most of the existing work simplifies the interaction between the operating speed of multiple trains and tractive/braking power. Furthermore, the interaction and mutually beneficial relationship between the traction system and power system are generally ignored.

The energy storage batteries are normally adopted in the rail traction power supply system, which can suppress the power fluctuation of the traction load and reduce the operating energy consumption of the rail trains. In [17], through the real-time data of power and position, the charging power of the energy storage devices can be dynamically adjusted to reduce the operating energy consumption of the traction system. But the study only considered the driving demand of a single train, and does not consider the demand response decision under different electricity prices. In [18], in considering the measured load data and power flow distribution of the traction substation, the braking energy recovered in the valley and the flat of the system load will be partially transferred to the peak of the system load. Through the coordinated control of the energy storage system, the peak power of the traction substation is reduced to achieve energy-saving operations. This work focuses on the impacts of charging/discharging power of the energy storage devices, while ignoring the interactions between the train operating state and the output of the energy storage device and the load of the traction system.

Inspired by the above-mentioned studies, this paper proposes a decision-making method for the coordinated demand response of a rail transit load and energy storage battery, considering driving comfort. This method can change the rail train load power by adjusting the driving speed under traction, cruising and braking conditions while satisfying the multi-train driving timetable and considering the requirements of train driving comfort. Meanwhile, this method aims to reduce the energy consumption cost of the rail transit system by controlling the charging/discharging power of the energy storage battery, thus realizing the peak-cutting and valley-filling of the power system. First, considering driving comfort, the cooperative operational mode between the rail train load and the energy storage battery is designed. Secondly, based on the load characteristics of the trains, operating modes and comfort requirements, the adjustable power range of the multi-track train load within a certain operating time is obtained. Based on this, considering the constraints of running time, driving speed limit, motor characteristics, etc., the model optimizes the speed trajectory curve of the rail train with the goal of the lowest operating energy cost of multi-rail transportation trains under two-part and TOU power prices. Finally, a numerical example analysis verifies the effectiveness of the proposed model.

II. Design of Decision Framework for Demand Response of Rail Transit Train System Considering Driving Comfort

A. Rail Transit Train Operations Considering Driving Comfort

The rail transit system coordinates the arrival and departure time of the trains at each station through pre-determined schedules. The train driving between stations usually includes four working conditions: traction, cruising, idling and braking, which correspond to the four processes of train acceleration, uniform speed operation, speed slowing and braking deceleration.

The train drives on the track line, and changes the operating conditions, which causes the train speed to change and influences the human body and physical discomfort. That is, the driving comfort would be changed. The driving comfort is primarily determined by the speed of the train and the spatial position of the track centerline.

As shown in Fig. 1, the track centerline refers to the line along the longitudinal line at the intersection O of the vertical line AB halfway from the outer track and the horizontal connection line CD of the two shoulder edges on the cross section of the track subgrade. The spatial position of the track centerline is represented by the line plane and the vertical section. The projection on the horizontal plane is the plane curve of the line and the projection on the vertical section

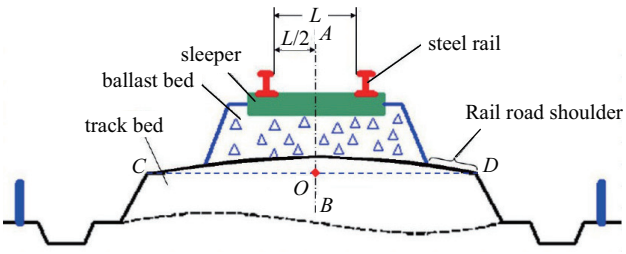

Fig. 1. Definition of track centerline.

is the vertical curve of the line. The train passes through the plane curve and the vertical curve at a certain speed, generating centrifugal acceleration, and the driving comfort of the train changes. On already-operated tracks, the line parameters are constant, and the size and direction of the train's running speed determines the driving comfort of the train.

The plane curve of the track line indicates the straight and curved changes of the track line on the horizontal plane, and the vertical curve indicates the slope change of the track line. When the train passes the plane curve, i.e., the curved line at high speed, the centrifugal acceleration changes, and the lateral comfort and vertical comfort of the train changes. When the train passes through the vertical curve, that is, going uphill or downhill at high speed, the vertical centrifugal acceleration changes, and the vertical comfort of the train changes.

Therefore, when the train passes through the plane curve or vertical curve of the track line, the running speed of the train is adjusted to meet the driving comfort requirements of the train operation under the condition of satisfying the running requirements of the train.

B. Demand Response Decision of Rail Transit System with Minimum Operational Energy Cost

In the rail traction power supply system for trains, the area between two consecutive traction substations represents a power supply interval. In order to meet the power requirements of trains, the electricity energy is transmitted by traction substation through the high-voltage transmission network to the AC or DC traction systems. For instance, the inter-provincial high-speed railway systems generally require the voltage to be reduced from 220 kV/110 kV to 27.5 kV AC traction network. Such reduction is from 35 kV to 1.5 kV (or 0.75 kV DC) for urban metro systems. Subsequently, the energy is fed into the electric trains via the traction system networks.

This coupling of the rail transit and power system is illustrated in Fig. 2. The generated power is returned to the traction substation through the running tracks and the backflow grid. When the trains brake, the generated regenerative energy is fed into the traction grid by the pantograph installed on the roof of the trains. When the train is driving between stations, the electrical energy is used by the traction and is returned by the braking. Therefore, the train generally serves as a load/source of the power system in a tractive/brake mode. The power network and railway network are coupled and mutually influenced.

The different operational conditions of rail train motors determine the form of electrical energy interaction. When the traction motor is in the electric mode, the train is in traction or cruising conditions, and it accelerates to start running or maintains a constant speed. At this time, the electric energy flows in the forward direction, which is absorbed and converted into kinetic energy from the traction network; when the traction motor is in the power generation mode, the train is in braking condition and decelerates. At this time, the electric energy flows in the reverse direction, and the kinetic energy generated by the train brakes is consumed by the auxiliary facilities of the train itself, with most of them being fed back to the traction network by the pantograph and absorbed by the adjacent trains in the same power supply section.

The power system implements an industrial price mechanism (two-part and TOU power prices) for urban rail transit systems, including capacity price and electricity price. Among them, the capacity electricity price is charged according to the maximum demand reported by the rail transit users, that is, according to the monthly maximum load value. When the maximum load of the rail transit exceeds the maximum demand, the excess is charged according to the penalty power price. The energy consumption is charged according to different prices at the peak, flat and valley of the system load.

The energy storage battery is installed on the low voltage side of the traction substation, and the load power of the traction substation is changed by controlling the charging and discharging power. On the one hand, the energy storage batteries are charged at the valley of the system load and discharged at the peak of the system load, which reduces the peak load of the train traction power supply system and the capacity electricity charges of the rail transit users. On the other hand, the energy storage batteries are charged when the electricity price is low, and discharged when the electricity price is high, which reduces the electricity cost of the rail transit users. Therefore, in the rail traction power supply system where the energy storage battery is installed, the energy consumption cost of the rail transit system can be minimized by adjusting the train speed trajectory and controlling the charging and discharging states of the energy storage batteries configured in the traction substation.

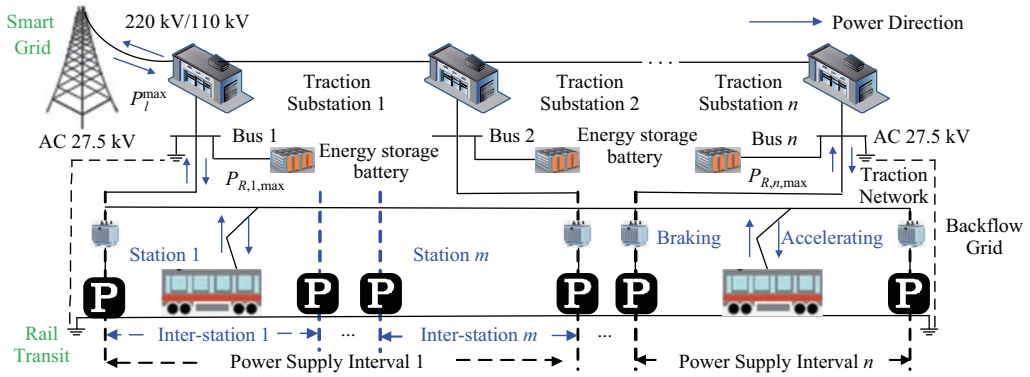

Fig. 2. Coupling of rail transit and power system.

III. Controllable Load Modelling of Multiple Trains in Satisfying Traffic Demand

There are three types of inter-provincial, inter-city and intra-city rail transit systems. The rail transit load has the characteristics of large adjustment capacity and slow adjustment speed, which can be used as a dispatchable resource in the demand side of power system. In this paper, by cooperating with the charging/discharging of the energy storage system, the optimal demand response of the rail traction power supply system is realized.

A. Load Modeling of A Single Train Traction Under Different Operating Conditions

The loading power of rail trains primarily includes the energy for the traction system and the auxiliary facilities. The auxiliary energy is typically constant, while the traction energy is determined by the operating conditions of the rail trains.

The characteristics of traction energy of rail trains in different operational states are illustrated in Fig. 3. Specifically, i) when the train is at the accelerating state, the electric energy is absorbed from the traction network. The acceleration is started to reach the required speed; ii) when the train is at the cruising state, it absorbs the electricity to overcome the resistance. The train can be moving at a constant speed; iii) when the train is at the coasting state, the electric energy is neither absorbed nor generated. The driving speed will be slowly decreased at this stage; and iv) when the train is at the braking state, the regenerative energy can be produced, which drives the motor to generate electricity that can be fed back into the traction network.

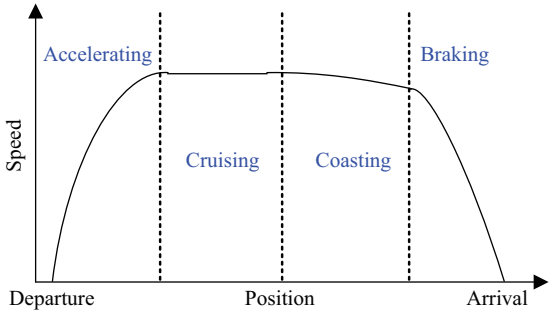

Fig. 3. Speed curves between stations under four operating conditions.

When the train is at the accelerating, cruising and braking operating conditions, the relationship between the driving speed and train loading power determined by tractive effort, braking force and resistance are expressed as:

$$P_{\mathrm{R},i,t}=\begin{cases}F_{\mathrm{q},i,t}v_{i,t}/\eta+P_{i,\mathrm{aux}}, & \text{Accelerating}\\ (f_{i,t}+w_{i,t})v_{i,t}/\eta+P_{i,\mathrm{aux}}, & \text{Cruising}\\ -F_{\mathrm{b},i,t}v_{i,t}\eta+P_{i,\mathrm{aux}}, & \text{Braking}\end{cases} \tag{1}$$

The tractive force of the train is produced by the motor in the same direction as the train, of which the characteristic curve is formulated as:

$$F_{\mathrm{q},i,t}=u_{\mathrm{f}}f(v_{i,t},E_i) \tag{2}$$

where $u_{\mathrm{f}}\in[0,1]$. The braking force of the train is generated by the motor in the opposite direction to the train, of which the characteristic curve is formulated as:

$$F_{\mathrm{b},i,t}=u_{\mathrm{b}}b(v_{i,t},E_i) \tag{3}$$

where $u_{\mathrm{b}}\in[0,1]$. For different types of trains, the characteristic curves of tractive and braking force can be referred to in [19].

The resistance of the train during the operating process consists of basic resistance and additional resistance. Additional resistance includes ramping resistance, curve resistance and tunnel resistance. The functional relationship between the basic resistance and the driving speed of the train is formulated as:

$$f_{i,t}=a^{\mathrm{r}}+b^{\mathrm{r}}v_{i,t}+c^{\mathrm{r}}v_{i,t}^2 \tag{4}$$

The ramp resistance is caused by the force of gravity when the train runs on the ramp. The ramp resistance is formulated as:

$$w_{i,\mathrm{q}}=q \tag{5}$$

Curve resistance is the additional frictional resistance generated by the wheel rim and the side of the rail when the train is running on the curve line. The curve resistance is formulated as:

$$w_{i,\mathrm{r}}=600/R \tag{6}$$

There is no formal test formula for tunnel resistance, and it can be ignored as compared to ramp resistance and curve resistance. Therefore, the additional resistance of the train is formulated as:

$$w_{i,t}=w_{i,\mathrm{q}}+w_{i,\mathrm{r}} \tag{7}$$

B. Node Load Power Modeling of the Traction Substation Considering Simultaneous Operation of Multiple Trains

If the train is represented as a power source, the power supply interval of the traction substation n contains I trains at the equivalent circuit is shown in Fig. 4. One traction substation governs a power supply interval, which are set at the same number. This paper only takes active power into account whereas the line impedance is neglected. The voltage of the low voltage side of the traction substation and the voltage of all trains is set as equal, i.e. $E=V_1=V_2=\cdots=V_I$.

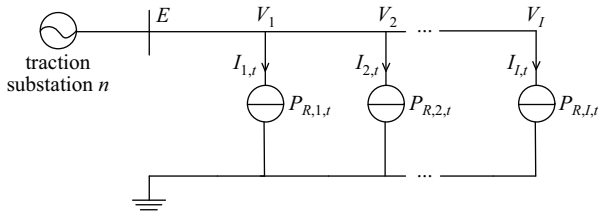

Fig. 4. Equivalent circuit in power supply interval with train.

If the traction network voltage is assumed to be nominal, the train loading power is determined by the train driving speed based on (1)–(4), i.e.

$$P_{\mathrm{R},n,\mathrm{t}}=\sum_{i\in\Omega_n}P_{\mathrm{R},i,t}(v_{i,t}) \tag{8}$$

The required loading power $P_{\mathrm{R},n,t}$ of all trains in the power supply interval n should be subject to the constraint of maximum power $P_{\mathrm{R},n,\max}$ provided by the traction network, i.e.,

$$P_{\mathrm{R},n,t} \le P_{\mathrm{R},n,\max} \tag{9}$$

It is strictly required to follow the planned schedules for the normal operation of rail trains. When the train is moving between stations, the speed can be controlled and adjusted according to certain requirements, as shown in Fig. 5.

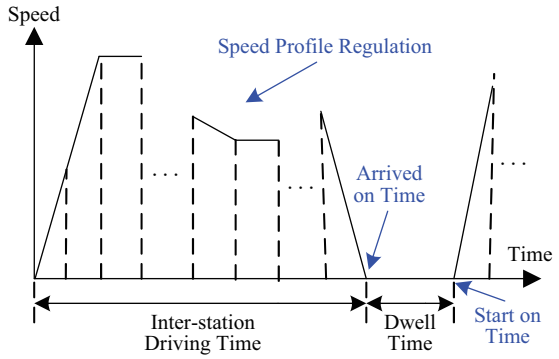

Fig. 5. Speed-time curve of controllable train.

The set of all sections in the rail transit network is denoted as $V = \{1, 2, \cdots, M\}$. A set of sections belonging to stations is denoted as Γ_{D}. Each section number in set Γ_{D} represents one station. The set of all sections within the jurisdiction of the power supply interval n is assumed as Γ_n.

If the train leaves section m at the speed of $v_{i,m}$ and maintains an uniform acceleration rate $a_{i,m,m'}$, the speed $v_{i,m'}$ of the train i to the next section m' is modeled as:

$$v_{i,m'} = \sqrt{2a_{i,m,m'}L_{m,m'} + v_{i,m}^2}, (m, m' \in V) \tag{10}$$

where m' is the section bus in a rail transit network connected to section m.

The accelerating process of a train can be influenced by the traction force, braking force and resistance, which determines the increase-and-decrease capability of the train speed. The maximum speed of the trains is restricted by the track construction. In order to ensure safe transportation, the speed and accelerating rate of the train should be subject to, i.e.,

$$0 \le v_{i,m} \le v_{\max}, \qquad (m \in V) \tag{11}$$

$$a_{\min} \le a_{i,m} \le a_{\max}, \qquad (m \in V) \tag{12}$$

The arrival speed of the train to the station must be 0. Thereby, the speed on the station section is intrinsically set as 0, i.e.,

$$v_{i,m} = 0, (m \in \Gamma_{\mathrm{D}}) \tag{13}$$

If the arrival time of train i to station section m is $t_{i,m}$, the driving time to the station section m' is:

$$t_{i,m'} = \begin{cases} t_{i,m} + \dfrac{L_{m,m'}}{\bar{v}_{i,m,m'}} + \Delta T_{i,m}, & (m \ne s_i, m' \in V) \\ t_{i,\mathrm{start}} + \dfrac{L_{m,m'}}{\bar{v}_{i,m,m'}}, & (m = s_i, m' \in V) \end{cases} \tag{14}$$

When the train is leaving the station, $\Delta T_{i,m}$ is the dwell time in station $m(m \in \Gamma_{\mathrm{D}})$; When the train passes other sections, $\Delta T_{i,m} = 0(m \notin \Gamma_{\mathrm{D}})$. When the train is moving in a straight line with uniform acceleration rate, the average driving speed between station sections m and m' is $\bar{v}_{i,m,m'} = (v_{i,m} + v_{i,m'})/2$.

In addition, the arrival time of train i is subject to the timetable constraint, i.e.,

$$t_{i,m} = T_{i,m}, (m \in \Gamma_{\mathrm{D}}) \tag{15}$$

Thereby, in order to meet the traffic demand of the rail trains (10)–(15), the driving speed of the train under the accelerating, cruising, coasting or braking states at time t is expressed as:

$$v_{i,t} = \begin{cases} v_{i,m} & \\ & t \in [t_{i,m} \quad t_{i,m} + \Delta T_{i,m}] \\ v_{i,m} + a_{i,m,m'}(t - \Delta T_{i,m} - t_{i,m}) & \\ & t \in [t_{i,m} + \Delta T_{i,m} \quad t_{i,m'}] \end{cases} \tag{16}$$

Equation (16) indicates the speed of train i at time t when it arrives at section m or travels between sections m and m'. When the train arrives or leaves the station section m, if $\Delta T_{i,m} \ne 0$, $v_{i,t} = v_{i,m} = 0$. Thus, the loading power of the traction substation n is the sum of the loading power requested by all the trains within the regulation region, i.e.,

$$P_{\mathrm{R},n,t} = \sum_{i \in \Omega_n} \sum_{m,m' \in \Gamma_n} \begin{cases} F_{\mathrm{q},i,t}(v_{i,t})v_{i,t}/\eta + P_{i,\mathrm{aux}}, & a_{i,m,m'} > 0 \\ [f_{i,t}(v_{i,t}) + w_{i,t}]v_{i,t}/\eta + P_{i,\mathrm{aux}}, & a_{i,m,m'} = 0 \\ -F_{\mathrm{b},i,t}(v_{i,t})v_{i,t}\eta + P_{i,\mathrm{aux}}, & a_{i,m,m'} < 0 \end{cases}$$
$$t \in [t_{i,m} \quad t_{i,m'}] \tag{17}$$

As a load, the train traction system absorbs power $P_{\mathrm{R},n,t}$ from the power grid through the traction substation under the condition of meeting the requirements of rail transit operations, i.e., (10)–(15). Under two-part and TOU prices, the driving speed of trains is adjusted on the basis of meeting the requirements of rail transit operations, so as to achieve the lowest cost of electricity purchase for the rail transit system.

C. Comfort Modeling of Trains Running on the Track

1) Train Comfort Model Considering Plane Curve and Vertical Curve

When the train passes the plane curve and the vertical curve of the track line at a certain speed, the driving comfort of the train produces a certain static change. This change is related to the train speed, the plane curve parameters (the radius, superelevation, length of the plane curve) and the vertical curve parameters (the radius, length of the vertical curve) and other factors.

When the train passes the plane curve and the vertical curve of the track line, the centrifugal acceleration of the train changes, i.e.,

$$a_{\mathrm{LX1},i,m} = \frac{v_{i,m}^2}{R_{\mathrm{H}}} - g\frac{H}{D}, a_{\mathrm{LX2},i,m} = \frac{v_{i,m}^2}{R_{\mathrm{s}}}, (m \in V) \tag{18}$$

The lateral comfort $\beta_{\mathrm{HX},i,m}$ of the train is determined by the centrifugal acceleration $a_{\mathrm{LX1},i,m}$, i.e.,

$$\beta_{\mathrm{HX},i,m} = a_{\mathrm{LX1},i,m}\frac{L_{\mathrm{H}}}{L}\cos\left(\frac{H}{D}\right), (m \in V) \tag{19}$$

The vertical comfort of the train is determined jointly by the centrifugal acceleration $a_{\mathrm{LX1},i,m}$ and $a_{\mathrm{LX2},i,m}$, i.e.,

$$\begin{cases} \beta_{\mathrm{CX1},i,m} = a_{\mathrm{LX1},i,m}\dfrac{L_{\mathrm{H}}}{L}\sin\left(\dfrac{H}{D}\right) \\ \beta_{\mathrm{CX2},i,m} = a_{\mathrm{LX2},i,m}\dfrac{L_{\mathrm{s}}}{L} \end{cases}, (m \in V) \tag{20}$$

According to "High-speed Railway Design Code (TB10621-2009)" in China, the vertical comfort $\beta_{\mathrm{CX},i,m}$ of train i passing section m without considering the track irregularities is:

$$\beta_{\mathrm{CX},i,m} = \beta_{\mathrm{CX1},i,m} + \beta_{\mathrm{CX2},i,m}, (m \in V) \tag{21}$$

2) Comfort Interval

When the train is driving on the track line of the plane curve and the vertical curve, the lateral comfort and vertical comfort levels are measured with reference to the IS02631 international standard. The measurement standards are shown in Table I below.

TABLE I
METRICS OF COMFORT LEVEL

Comfort level	Comfort zone	Evaluation results
Level 1	< 0.315	Extremely comfortable
Level 2	(0.315, 0.5]	Very comfortable
Level 3	(0.5, 0.8]	Comfortable
Level 4	(0.8, 1.25]	Uncomfortable
Level 5	(1.25, 2]	Very uncomfortable
Level 6	> 2	Extremely uncomfortable

The driving comfort of train i should meet the comfort requirements, i.e.,

$$\beta_{\mathrm{HX},i,m}, \beta_{\mathrm{CX},i,m} \in (a, b], (m \in V) \tag{22}$$

When the train is in an extremely comfortable state, $a = 0$, $b = 0.315$; When the train is in a very comfortable state, $a = 0.315$, $b = 0.5$; When the train is in a comfortable state, $a = 0.5$, $b = 0.8$. The specific value can be set according to the actual comfort requirements. The comfort interval selected in this paper is (0, 0.8].

IV. OPTIMAL DECISION-MAKINGS FOR RAIL TRANSIT LOAD AND ENERGY STORAGE BATTERY

A. Objective Function

The rail transit system is connected to the power system as a large industrial load, and the energy consumption fee is charged according to the two-part and TOU prices. The energy storage batteries charge at the valley of the system load and discharge at the peak of the system load, that is, the energy storage batteries absorb electrical energy from the power grid at the valley of the system load and it discharges at the peak of the system load, thereby reducing the cost of purchasing electricity for rail transit trains.

Through determining the speed trajectory of the train and the charge and discharge power of the energy storage batteries, the optimization model that aims at minimizing capacity and electricity costs achieves the lowest cost of electricity purchase for the rail system and the peak-cutting and valley-filling of the power system. The objective function of the optimal cooperative demand response of the rail transit load and energy storage battery is:

$$\begin{aligned} C = \min_{(v_{i,t}, P_{\mathrm{E},n,t})} & \sum_{n=1}^{N}\sum_{t=1}^{\mathrm{T}}\left((P_{\mathrm{R},n,t} + P_{\mathrm{E},n,t})e_{\mathrm{t}} + k|P_{\mathrm{E},n,t}|\right) \\ & + e_{\mathrm{s}}S + e_{\mathrm{z}}\left[\max\sum_{n=1}^{N}\sum_{t=1}^{\mathrm{T}}(P_{\mathrm{R},n,t} + P_{\mathrm{E},n,t}) - S\right] \end{aligned} \tag{23}$$

where C means that the cost of purchasing electricity for the rail train system is the least; the positive value of $P_{\mathrm{E},n,t}$indicates the charging power of the energy storage battery at time instant t on node n, and the negative value indicates the discharge power.

B. Constraints

The traction load of a rail train is determined by the speed trajectory under the constraints of meeting the operational schedule. Decision variables, i.e. the speed trajectory of the train and the charge and discharge power of the energy storage batteries, are subject to a series of constraints, such as the physical characteristics of the train traction network and the rail transit operational requirements, which include i) maximum power available from the traction electric network as expressed in (9); ii) the speed and accelerated speed limitation of rail trains for driving safety, as expressed in (11) and (12); iii) the driving time of rail trains as expressed in (15); and iv) the driving comfort of rail trains as expressed in (22). In addition, the system also needs to meet the following constraints to realize the coordinated operations of rail trains and energy storage devices.

1) System Power Balance

$$\sum_{n=1}^{N} P_{\mathrm{G},n,t} = \sum_{n=1}^{N} P_{\mathrm{E},n,t} + \sum_{n=1}^{N} P_{\mathrm{R},n,t} \tag{24}$$

2) Upper And Lower Bounds of the Output Power of Energy Storage Batteries

$$P_{\mathrm{E},n}^{\min} < P_{\mathrm{E},n,t} < P_{\mathrm{E},n}^{\max} \tag{25}$$

3) The Capacity of Energy Storage Batteries Limits

$$\begin{cases} S_{n,t}^{\mathrm{SOC}} = S_{n,t-1}^{\mathrm{SOC}} + P_{\mathrm{E},n,t}\Delta t / B_{n,\mathrm{E}}^{\mathrm{Cap}} \\ S_{n,\min}^{\mathrm{SOC}} \le S_{n,t}^{\mathrm{SOC}} \le S_{n,\max}^{\mathrm{SOC}} \end{cases} \tag{26}$$

4) Transmission Line Thermal Limits

$$P_{\mathrm{l}} < P_{\mathrm{l}}^{\max} \tag{27}$$

C. Solver

The constructed optimization model of rail trains and energy storage battery comprises linear equality constraints (1), (8), (13), (15), (17) and (24), linear inequality constraints (9), (11), (12), (22) and (25)–(27), nonlinear equality constraints (4), (7), (10) and (18)–(21). This model is a typical mixed-integer nonlinear programming problem. In this paper, the branch and bound algorithm is deployed to solve the proposed model by employing the commercial solver CPLEX on MATLAB.

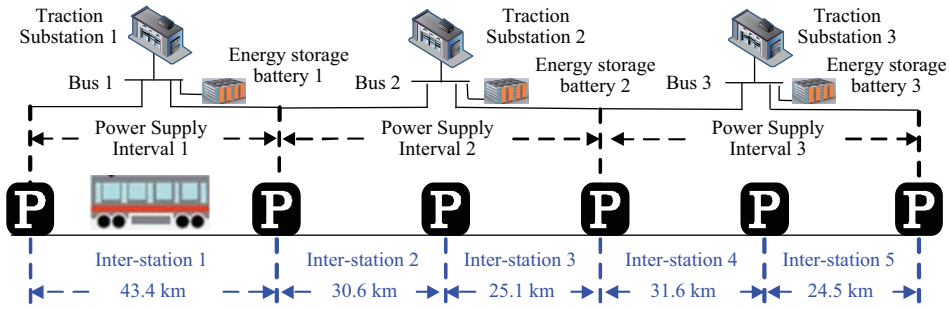

Fig. 6. Traction power supply system of the rail transit.

V. Numerical Simulation

A. Parameter Settings

A high-speed railway with a total length of 155.4 km has 3 traction substations and 6 stations. The traction power supply system is shown in Fig. 6. The maximum capacities of the traction substations are 35 MW, 40 WM and 40 MW, respectively. The energy storage batteries are installed on the low-voltage sides of the three traction substations, with capacities of 10 MW, 11 MW, and 11 MW, respectively.

The unit operation and maintenance costs of the energy storage batteries are 1×10^{-1} yuan/(kW·h). The capacity electricity price of rail transit users is 40 yuan/kW/month, and the penalty electricity price is 80 yuan/kW/month. The TOU power price is shown in Table II, and the maximum demand reported is 96 MW. Here, the CRH2 train is selected for simulation calculation, and the relevant parameters of the train are shown in Table III.

TABLE II
Electricity Price in Different Periods

Parameter	Time	Value (yuan/(kW·h))
The valley of system load	0:00–8:00	0.3139
The flat of system load	12:00–17:00, 21:00–24:00	0.6418
The peak of system load	8:00–12:00, 17:00–21:00	1.0697

TABLE III
Related Parameters of Rail Trains

Parameter	Value
Train mass (t)	200
Maximum operational speed (km/h)	300
Maximum accelerated speed (m/s^2)	0.5
Minimum accelerated speed (m/s^2)	-0.5
Rated power (MW)	10
Load power of auxiliary equipment (MW)	0.2
Energy conversion efficiency	0.85
Basic resistance force per unit mass (N/KN)	$1.12 + 0.00542\ v_{i,t} + 0.000146\ v_{i,t}^2$

The speed trajectory of the train and the charge/discharge power of energy storage batteries are optimized by the proposed model on that day before the operation of the rail transit system according to the operation timetable of the train. The simulation is implemented by MATLAB 7.0, and runs on a personal computer with Inter cure i5-7300 CPU and 8 GB RAM. The average calculation time for solving the optimization model is 34.35 s, which meets the time requirements of dispatching the actual speed trajectory of the train and the actual charge and discharge power of energy storage batteries in practical applications.

B. Optimal Dispatching Result of the Train Traction Power Supply System

With the aid of the optimization model mentioned in this paper, the daily electricity purchase cost before and after the installation of energy storage equipment in the train traction power supply system in August is shown in Fig. 7. After the optimization, the cost of purchasing electricity for the rail transit system drops the most on the 21st, a total decrease of 57.56 thousand yuan, a decrease of 4.95%. In the whole month, the total cost of electricity purchase is reduced by 1,460.71 thousand yuan, and the total cost of electricity purchase is reduced from 33.64 million yuan to 32.18 million yuan, a decrease of 4.34%.

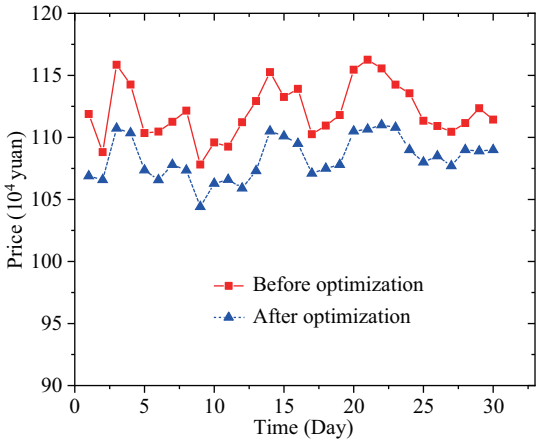

Fig. 7. Daily power purchase cost before and after the installation of energy storage batteries in the train traction power supply system.

After the energy storage battery is connected to the traction power supply system of the train, the peak value of electricity load is reduced, and the actual electricity load is prevented from exceeding the maximum demand reported by rail transit users. At the same time, the energy storage battery is low-charged and high-discharged, which reduces the electricity cost. The load curve before and after the installation of the energy storage battery in the train traction power supply system on a certain day in August is shown in Fig. 8.

At 8:40, the peak system load decreases from 99.26 MW

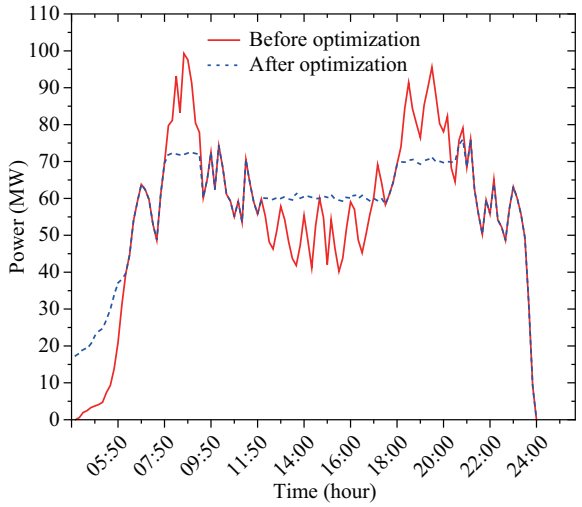

Fig. 8. The load curve before and after the optimization of the train traction power supply system within 24 h.

to 71.9 WM; at 0:00, the system load valley increases from 0 MW to 17.32 WM. In the train traction power supply system, by controlling the charging and discharging power of the energy storage battery and the train speed trajectory, the load curve becomes smooth and stable.

At the valley and flat stages of the system load (i.e. time slots of 0:00–8:00 and 12:00–17:00), the energy storage battery is in a charged state, absorbing 39.78 MW·h of electricity at 0:00–8:00, and absorbing 42.64 MW·h of electricity at 12:00–17:00. At the peak of system load (time slots of 8:00–12:00 and 17:00–21:00), the energy storage battery is in a discharged state, and the electrical energy is released, 37.92 MW·h at 8:00–12:00; and 42.5 WM·h of electrical energy is released at 17:00–21:00.

After the optimization, the train traction power supply system reduces the electricity cost by 38.16 thousand and the capacity electricity cost by 12.90 thousand yuan. The total cost of electricity purchase on the same day decreases from 1.10 million yuan to 0.93 million yuan, a decrease of 4.61%.

C. Optimal Result of Train Speed Trajectory

The experimental settings are shown in Table IV, and the optimization results of the train considering different operating characteristics are compared. The trajectory optimization results for the trains between stations 1 and 2 at the peak of system load are shown in Fig. 9, and the trajectory optimization results of trains at the valley of system load are shown in Fig. 10. The curve between stations 1 and 2 is similar, focusing on the comparative analysis of the train speed trajectory of station 1.

TABLE IV
EXPERIMENTAL SETTINGS

Cases	Description
1	Energy storage and driving comfort are not considered
2	Consider energy storage, not driving comfort
3	Both energy storage and driving comfort are considered

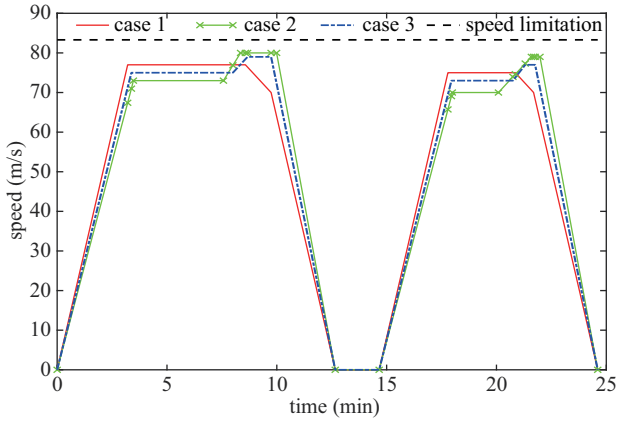

Fig. 9. The speed trajectory of rail trains at the peak of system load.

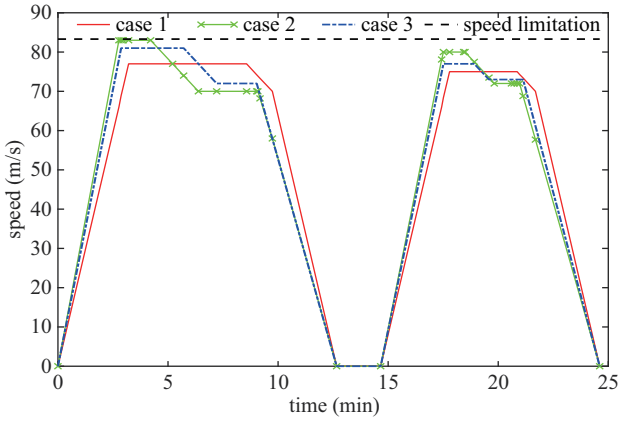

Fig. 10. The speed trajectory of rail trains at the valley of the system load.

1) Optimal Result of Train Speed Trajectory at the Peak of the System Load

In order to illustrate the impact of energy storage batteries on the speed trajectory of the train during peak hours, without considering the driving comfort, the speeds of the train without energy storage batteries installed in Case 1 and the train with energy storage batteries installed in Case 2 are compared and analyzed in Fig. 9.

At 0–2.5 min, the speed of the train in Case 1 is accelerated from 0 m/s to 77 m/s, and then the speed of 77 m/s is kept unchanged, and the train in Case 2 is accelerated to 73 m/s with a smaller acceleration than Case 1 and remains unchanged. In the case of acceleration, the load power in Case 2 is lower than Case 1 by 1.2 MW. At 2.5–8 min, the trains in Case 1 and Case 2 are in cruise mode, and the load power in Case 2 is reduced by 0.6 MW compared to Case 1. At 8–11 min, due to the same inter-station running time, the train in Case 2 accelerates to 80 m/s and remains unchanged. The power of the train during acceleration is increased by 0.32 MW compared to Case 1. At 11–12 min, the train in Case 2 decelerates to 0 m/s with a greater acceleration, which produces greater braking regenerative power than Case 1. Compared to Case 1, in order to adjust the load power more effectively, the load curve of the train traction power supply system becomes smooth in Case 2, and the cost of purchasing electricity per hour per train is reduced by 574.86 yuan.

As compared to Case 2, Case 3 illustrates the impact of driving comfort on the train speed trajectory. The cruise speed of Case 3 is 79 m/s, which is smaller than Case 2 at 8–11 min. In order to improve driving comfort, the change range of speed in Case 3 is smaller than that in Case 2, and the change range of load power in Case 3 is also smaller than that in Case 2 under the condition of constant running time between stations. The cost per hour of electricity purchase for each train in Case 3 is 361.96 yuan lower than that in Case 1.

2) Optimal Result of Train Speed Trajectory at the Valley of the System Load

In order to further illustrate the effect of energy storage on the speed trajectory of the train at the valley of the system load, without considering the driving comfort, the operating state of the train without energy storage batteries in Case 1 and the operating state of the train with energy storage batteries in Case 2 are compared and analyzed in Fig. 10.

At 0–2.5 min, the speed of the train accelerates from 0 m/s to 77 m/s, and then maintains the driving speed of 77 m/s unchanged in Case 1. In Case 2, the train accelerates to 83 m/s at a higher acceleration than Case 1 and remains unchanged. In the case of acceleration, the load power in Case 2 is increased by 2.3 MW compared to Case 1. At 2.5–8.5 min, the train in Case 1 is in cruise mode, and the train in Case 2 has passed through 3 modes, namely cruise, brake and cruise. In the first cruising condition, the load power in Case 2 is increased by 0.24 MW as compared to Case 1. In braking conditions, the load power in Case 2 is reduced by 3.21 MW as compared to Case 1. In the second cruise condition, the load power in Case 2 is reduced by 0.62 MW as compared to Case 1. At 10–12 min, the train in Case 2 decelerates to 0 m/s with a smaller acceleration as compared to Case 1, which produces less braking regenerative power as compared to Case 1. Under the condition that the driving time between stations is constant, in order to adjust the load power more effectively, the load curve of train traction power supply system in Case 2 becomes smoother than Case 1. The hourly electricity purchase cost of each train of case 2 is 411.49 yuan lower than case 1.

As compared to Case 2, Case 3 illustrates the restriction and influence of driving comfort on the train speed trajectory. At 0–2.5 min, the speed of the train in Case 3 accelerates from 0 m/s to 80 m/s, and then maintains the speed of 80 m/s unchanged. The acceleration and maximum speed of the train in Case 3 are less than Case 2, and in the case of acceleration, the load power in Case 3 is lower than that in Case 2 by 1.1 MW. In order to improve driving comfort, the cruising speed and adjustment power in Case 3 is smaller than Case 2. The cost per hour of electricity purchase for each train in Case 3 is 285.1 yuan lower than Case 1.

VI. Conclusion

This paper proposes an optimization model for demand response decision-makings for the traction power supply system according to the two-part price and TOU power price. The proposed model aims to minimize the energy consumption cost of rail transit trains by taking into account driving comfort and train power regulation capabilities. This model reduces the cost of electricity purchased by the rail transit users by controlling the train speed trajectory and charging/discharging power of energy storage batteries. Through a comprehensive case study of a traction power supply system, the effectiveness and feasibility of the proposed model are verified. Furthermore, the optimal demand response of the traction power supply system will be investigated while simultaneously changing the train operational diagram and train running speed trajectory in our future study.

References

[1] H. J. Sun, J. J. Wu, H. N Ma, X. Yang, and Z. Y. Gao, "A bi-objective timetable optimization model for urban rail transit based on the time-dependent passenger volume," *IEEE Transactions on Intelligent Transportation Systems*, vol. 20, no. 2, pp. 604–615, Feb. 2019.

[2] China National Railway Corporation LTD. (2019, Mar.). Statistics and analysis of urban rail transit in 2018. China National Railway Corporation LTD, China. [Online]. Available: https://www.camet.org.cn/tjxx/3101.

[3] H. T. Hu, Z. Zheng, Z. Y. He, B. Wei, K. Wang, X. W. Yang, and W. J. Wei, "The framework and key technologies of traffic energy internet," *Proceedings of the CSEE*, vol. 38, no. 1, pp. 12–24, Jan. 2018.

[4] Q. Z. Li, X. J. Wang, X. H. Huang, Y. Zhao, Y. W. Liu, and S. F. Zhao, "Research on flywheel energy storage technology for electrified railway," *Proceedings of the CSEE*, vol. 39, no. 7, pp. 2025–2033, Apr. 2019.

[5] H. M. Yang, J. Zhang, J. Qiu, S. H. Zhang, M. Y. Lai, and Z. Y. Dong, "A practical pricing approach to smart grid demand response based on load classification," *IEEE Transactions on Smart Grid*, vol. 9, no. 1, pp. 179–190, Jan. 2018.

[6] H. M. Yang, Q. Yu, J. P. Liu, Y. W. Jia, G. Y. Yang, E. Ackom, and Z. Y. Dong. "Optimal wind-solar capacity allocation with coordination of dynamic regulation of hydropower and energy intensive controllable load," *IEEE Access*, vol. 8, pp. 110129–110139, Jun. 2020.

[7] X. Yang, X. Li, B. Ning, and T. Tang, "A survey on energy-efficient train operation for urban rail transit," *IEEE Transactions on Intelligent Transportation Systems*, vol. 17, no. 1, pp. 2–13, Jan. 2016.

[8] G. M. Scheepmaker, P. J. Pudney, A. R. Albrecht, R. M. P. Goverde, and P. G. Howlett. "Optimal running time supplement distribution in train schedules for energy-efficient train control," *Journal of Rail Transport Planning & Management*, vol. 14, pp. 100180, Jun. 2020.

[9] M. Khodaparastan, A. A. Mohamed, and W. Brandauer, "Recuperation of regenerative braking energy in electric rail transit systems," *IEEE Transactions on Intelligent Transportation Systems*, vol. 20, no. 8, pp. 2831–2847, Aug. 2019.

[10] S. Lin, D. Huang, A. M. Wang, Y. J. Huang, L. P. Zhao, R. Luo, and G. T. Lu, "Research on the regeneration braking energy feedback system of urban rail transit," *IEEE Transactions on Vehicular Technology*, vol. 68, no. 8, pp. 7329–7339, Aug. 2019.

[11] J. T. Haahr, D. Pisinger, and M. Sabbaghian, "A dynamic programming approach for optimizing train speed profiles with speed restrictions and passage points," *Transportation Research Part B*: *Methodological*, vol. 99, pp. 167–182, May 2017.

[12] H. Gao, Y. D. Zhang, J. Guo, and K. H. Li, "The two-stage optimization method of train energy-efficient operation based on dynamic programming," *Journal of Southwest Jiaotong University*, Apr. 2020. Online: http://kns.cnki.net/kcms/detail/51.1277.u.20200426.1044.002.html.

[13] S. G. Wei, X. H. Yan, B. G. Cai, and J. Wang, "Multiobjective optimization for train speed trajectory in CTCS high-speed railway with hybrid evolutionary algorithm," *IEEE Transactions on Intelligent Transportation Systems*, vol. 16, no. 4, pp. 2215–2225, Aug. 2015.

[14] Z. X. Xia, "Research of evaluation method on riding comfort of high-speed train," M.S. thesis, Department of Mechanical Engineering and Automation, Northeastern University, Shenyang, China, 2010.

[15] Y. B. Zhang, Z. Q. Chen, J. M. Wang, and P. D. Wu, "Research on the comfort control technology of the ATO system in high-speed railway," *Journal of Railway Engineering Society*, vol. 36, no. 3, pp. 67–71, Mar. 2019.

[16] H. Y. Wang, "Study on the comfort evaluation mechanism and application of high-speed trains," Ph.D. dissertation, Department of Traffic Information Engineering and Control, Lanzhou Jiaotong University, Lanzhou, China, 2014.

[17] H. Xia, Z. P. Yang, Z. H. Yang, F. Lin, and X. Y. Li, "Control strategy of supercapacitor energy storage system for urban rail transit based on operating status of Trains," *Transactions of China Electrotechnical Society*, vol. 32, no. 21, pp. 16–23, Nov. 2017.
[18] W. L. Deng, C. H. Dai, C. B. X. Han, and W. R. Chen, "Back-to-back hybrid energy storage system of electric railway and its control method considering regenerative braking energy recovery and power quality improvement," *Proceedings of the CSEE*, vol. 39, no. 10, pp. 2914–2923, May 2019.
[19] Train Traction Calculation Procedure, China Standard TB/T 1407–1998, 2006.

Hongming Yang received the M.S. degree in Electrical Engineering from Wuhan University in 1997, and the Ph.D. degree in Electrical Engineering from Huazhong University of Science and Technology in 2003. She was a Research Associate at the Hong Kong Polytechnic University in 2009–2010, and also a Research Fellow at the University of Newcastle in 2013–2014. Currently, she is a full Professor at Changsha University of Science and Technology. Her research interests include power system analysis and power markets.

Wangda Shen received the B.S. degree in Electrical Engineering at Changsha University of Science and Technology, Changsha, China, in 2018. Currently, he is working toward the M.S. degree in Electrical Engineering at Changsha University of Science and Technology, Changsha, China. His research interests include electric vehicle and power system analysis.

Qian Yu received the M.S. degree in Industry & Business Administration at Guilin university of technology, Guilin, China, in 2016. She is currently pursuing the Ph.D. degree in Industry & Business Administration at the School of Economics and Management at Changsha University of Science and Technology, Changsha, China. Her research interests include renewable energy permeation and power system optimization.

Junpeng Liu received the B.S. degree in Electrical Engineering at Henan University of Technology, Zhengzhou, China, in 2018. Currently, he is working toward the M.S. degree in Electrical Engineering at Changsha University of Science and Technology, Changsha, China. His research interests include electricity market operations and electric vehicles.

Yizhe Jiang received the B.S. degree in Electrical Engineering at Changsha University of Science and Technology, Changsha, China, in 2018. Currently, he is working toward the M.S. degree in Electrical Engineering at Changsha University of Science and Technology, Changsha, China. His research interests include internet of things in power systems.

Emmanuel Ackom received the Ph.D. degree in Environment and Resource Management at the Brandenburg University of Technology (BTU), Germany, in 2005, through the Interdisciplinary Environment and Resource Management Program. He is currently a Senior Energy and Climate Expert with the UNEP DTU Partnership, Technical University of Denmark. His research interests include the intersection of clean energy policy and technologies, socio-economic development, and environmental sustainability with a particular emphasis on developing countries.

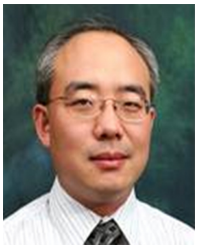

Zhao Yang Dong (F'17) received the M.S. degree in Electric Drive and Automation at Tianjin University, Tianjin, China, in 1995. And he received the Ph.D. degree in Electrical and Information Engineering at the University of Sydney, Australia, in 1999. He is currently a SHARP Professor at the University of NSW, Australia. His immediate role is Professor and Head of the School of Electrical and Information Engineering at the University of Sydney. His research interests include the smart grid, power system planning, power system security, load modeling, renewable energy systems, electricity market, and computational intelligence and its application in power engineering. Professor Dong is an editor of the IEEE Transactions on Smart Grid, IEEE Power Engineering Letters, and IET Renewable Power Generation.